Article

Not peer-reviewed version

# Some Next-Generation of Spindle Intelligence: Real-Time Condition Monitoring and Diagnosis

Claudiu Bisu , Adrian Olaru * , Serban Olaru , Niculae Mihai , Hussain Waleed

Posted Date: 23 April 2026

doi: 10.20944/preprints202604.1651.v1

Keywords: intelligent spindle; monitoring and diagnosis; acceleration; envelope acceleration; BDSVM; CNN

*Article*

# Some Next-Generation of Spindle Intelligence: Real-Time Condition Monitoring and Diagnosis

**Claudiu Bisu [1], Adrian Olaru [1,*], Serban Olaru [2], Niculae Mihai [3] and Hussain Waleed [1]**

[1] National University for Science and Technology Politehnica Bucharest
[2] Military Equipment and Technology Research Agency
[3] Concordia University, Montreal, Canada and Techno Accord CNC machine-tools company, Leuval, Canada
* Correspondence: aolaru_51@ymail.com; Tel.: +40723852628.

## Abstract

As the era of Industry 4.0 (i.e., the fourth-generation industrial revolution) develops, machine tools in particular are becoming interconnected, forming a collaborative community in smart factories. "Smart manufacturing" is becoming the norm, in a world where intelligent machines, systems, and networks are able to exchange information between them and respond independently, with autonomy to information, with the goal to manage industrial production processes. An important challenge is the transformation of traditional machines into intelligent machines, respectively intelligent or smart spindle. The purpose of this paper is to analyze the spindle using the intelligent models in in-situ conditions. The historical evolution, recent challenges and future trends of machine tool spindles were analyzed, noting that further development would be necessary to enable sensor/AI module integration to make the spindle unit an inherent quality assurance system. This study proposes a deep learning-based approach to spindle health monitoring based on multi sensor vibration signal analysis. The two proposed AI methods is based on the analysis of acceleration and synchronous envelope vibrations by demodulating the signal based on the Hilbert transform to identify critical bearing defects and specific defects at high frequencies.

**Keywords:** intelligent spindle; monitoring and diagnosis; acceleration; envelope acceleration; BDSVM; CNN

---

## 1. Introduction

The importance of spindle monitoring and diagnosis is well know, representing one of the priority research goals in the field of machine tools, especially in the case of high speeds and recent motorized technologies [1]. The need to use high-speed is not just a technological option, but a necessity imposed by the current requirements of the global market: speed, precision and low cost [2].The condition of the spindle determines the quality of processing and the performance of machine tools, but also their lifespan [3]. The complexity of vibration transmissibility, the multitude of vibration sources, as well as their coupling under severe operating conditions, make the diagnostic process limited or even produce large errors. The automation of the diagnostic process through Artificial Intelligence (AI)/Machine Learning is still maturing for ultra-precise applications [4-6]. In the last decade, a series of AI methods and algorithms have been presented, used in research and proposed for exploitation [7-8]. However, the multitude of factors in the field, in the industrial environment, makes the process need more maturity. Recent AI models have evolved from simply detecting anomalies to predicting future trends and generating synthetic data to compensate for the lack of defects samples. One of the biggest limitation is the lack of real, labelled data sets, real spindle failures are rare, industry data is difficult to obtain, many studies use experimental laboratory data [7-9]. Most AI models are based on this laboratory data, were conditions are bench-top, without the technical constraints and real life existing in industry. Operating conditions are increasingly severe, requiring the emergence of innovative solutions that are based on a coupling of several techniques,

 doi:10.20944/preprints202604.1651.v1



from signal acquisition to monitoring, diagnosis, algorithms for identification, decision and control [10]. The machine tool is a complex of components and processes where the spindle/ motor-spindle are the main actor, the one that provides the main cutting movement, the cutting speed [11]. A motor-spindle is the basic components of the next generation of intelligent/smart machine tools in the era of Industry 4.0 [11-12].

The purpose of this paper is to analyze the spindle using the intelligent models in in-situ conditions. Different AI methods are applied for a motor spindle to provide a concrete perspective of the latest generation technology regarding the monitoring, control, autonomy of the condition control, cutting process, the design of intelligent structures in the future machine-tools and smart factories [13-17].

A new integrated concept for motor-spindles is proposed, with decision-making autonomy adapted to the multifunctional requirements of the latest generation machine-tools compatible with Industry 4.0 [13]. Research carried out to support the future development of spindles includes monitoring and control of tool condition, noise in the cutting process, spindle vibration compensation, temperature control, dynamic spindle balance and increasing the degree of decision-making autonomy of smart machine tools with the help of specific modules [10]. Future trends from conventional spindle to smart spindles are analyzed from various perspectives [9-10]. The transition from a classic monitoring system to an integrated autonomous system offers the practical conditions for transformation into an intelligent spindle. Intelligent spindles can be described as spindles with autonomous sensing, decision-making and control capabilities, which guarantee an optimal machining process and reliable machining operations. Traditional spindles only have the ability to passively follow and react to operators' commands, even when the assigned task is not suitable for their current conditions. Smart spindles should be able to actively suggest the planning of various tasks and adjust or modify operational parameters, in order to optimize machining processes and ensure the efficient use of the spindle. In this context, the correct choice of the AI model, the accuracy of this collected data and the optimization of decision parameters are the main condition underlying an autonomous diagnosis.

The multitude of factors and their complexity can directly influence the operating condition of the spindle and, implicitly, the quality of the cutting process and the workpiece [18], making it absolutely necessary to monitor the condition, including the evolution of wear and bearing defect, before it fails catastrophically, leading to major damage to the component elements and the machine, as well as to production losses [18].

The transformation of a classic spindle motor into an intelligent spindle motor represents a scientific challenge considering the complex set of processes. In this context, a methodology is substantiated for the transfer to artificial intelligence techniques

## 2. Substantiation and Methodology

However, the spindle motor is a key component of a machine tool, ensuring its performance despite a complex behavior [10, 19]. Spindle motor condition monitoring is also an important issue due to the high maintenance costs in high-speed machining (HSM). This issue belongs to the broader scientific field of condition-based maintenance of rotating machines. The most common technique consists of detecting a fault by analyzing vibrations measured by transducers and sensors fixed at key positions on the spindle. In the current context of digitalization, conditioned by increased productivity and reduced downtime, the performance and reliability of the spindle are subject to a long development process, moving from the monitored spindle phase to the intelligent spindle phase, which provide diagnostics but also make decision autonomously [18]. Consequently, intelligent spindles will acquire knowledge of adjusting/modifying the various parameters of the cutting process through self-learning, in the deep learning variant, rather than following the rules set by operators in advance [10].

An integrated concept of intelligent spindles is presented in Fig. 1. Compared with conventional spindles, the intelligent spindles must possess new features, new modules, which ensure the increase of autonomy, self-learning, compatibility and maintainability. In order to design and build intelligent

 doi:10.20944/preprints202604.1651.v1



spindles, emphasis should be placed on the development of key technologies, intelligent modules, which include detection, autonomous decision-making and active control [5,20-21].

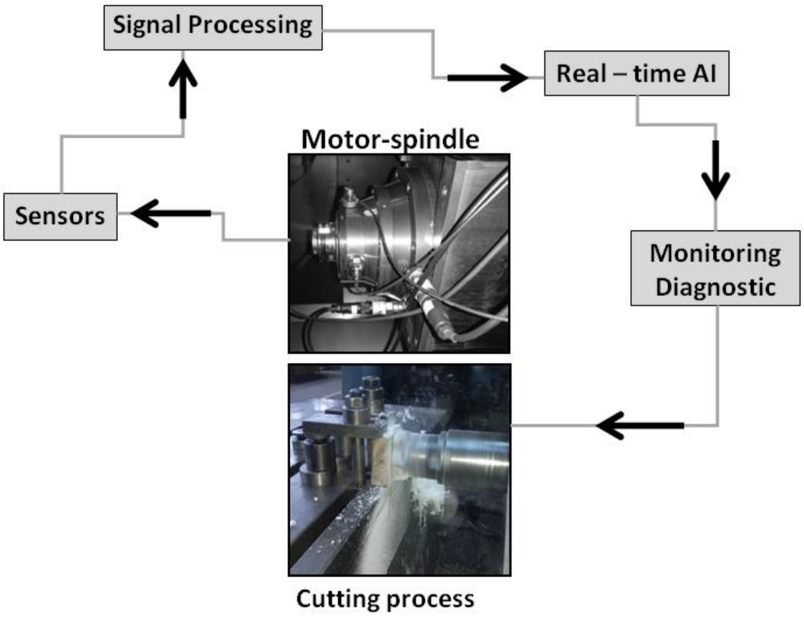


**Figure 1.** An integrated concept of one intelligent spindle monitoring and diagnosis.

The measured and query signals are imported into the decision-making and control modules as inputs. In the decision-making module, the measured signals are analyzed by advanced signal processing techniques and stored for the application of deep learning in future actions. The features representing the machining process state are extracted and then fed into pattern recognition algorithms for vibration detection/prediction. In the control module, vibration signals are fed into the vibration controller as feedback, and parameters such as spindle speed and temperature are provided to the controller to achieve the self-adaptive response [10]. The use of real data, collected directly from the machine, provides the premises for obtaining a specific model, applying a highly accurate algorithm. For a relevant AI model, a post-processing of the signals is required so that the key parameters for the model can be provided. The signals are obtained from the spindle sensors and then processed according to the diagram in figure 2. With post-processing, the data is provided to the real-time AI model where, based on the selected criteria, the necessary data is obtained that represents the new inputs in the cutting process. Figure 3 describes the post-processing monitoring and diagnosis method, based on fault detection in both the low and high frequency ranges. The application of SEA Synchronous Envelope Analysis [18, 22] offers the identification of bearing-specific faults, allowing a quantitative and qualitative assessment of their evolution. In bearing analysis, the input signal is not a simple sinusoid, but a complex mixture of periodic pulses, structural resonances, and noise [23].

Preprints.org (www.preprints.org) | NOT PEER-REVIEWED | Posted: 23 April 2026 doi:10.20944/preprints202604.1651.v1



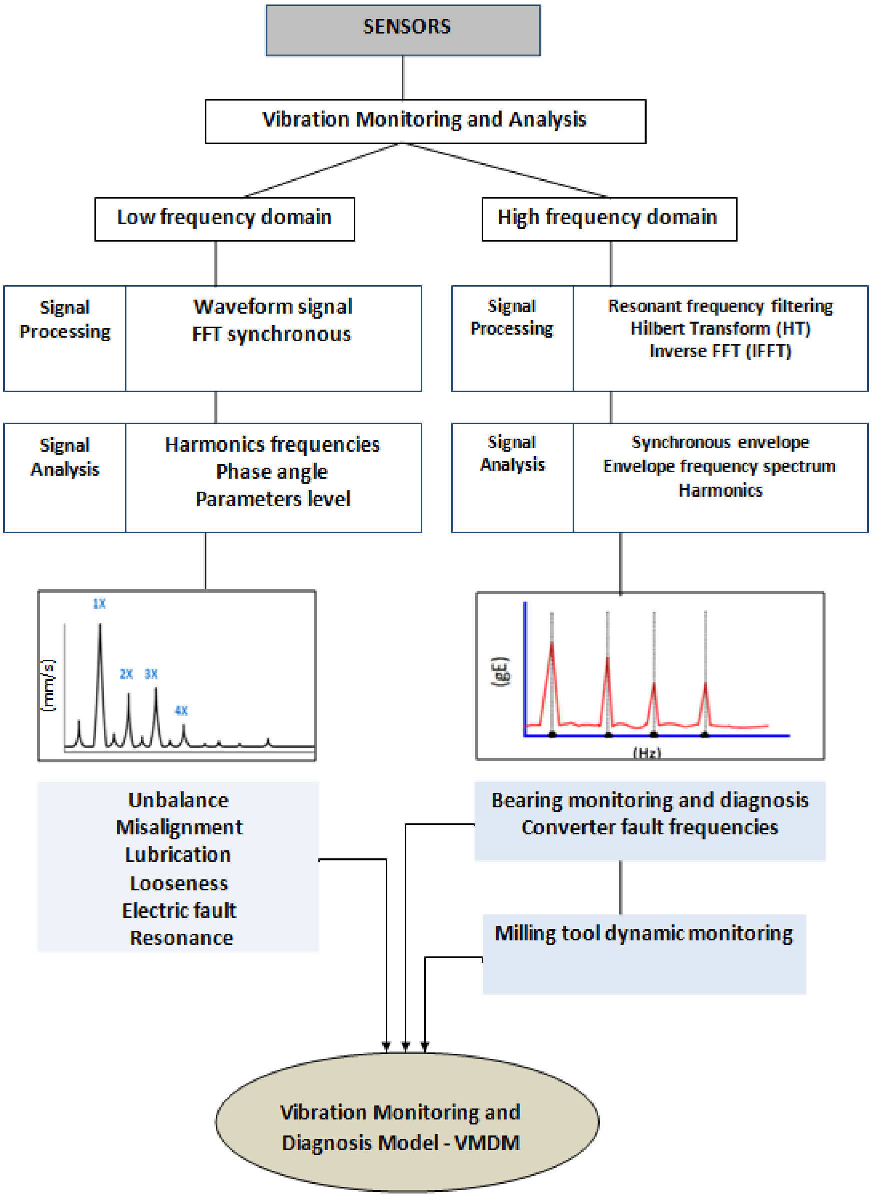


**Figure 2.** Monitoring and diagnosis model based on processing signal using Synchronous Envelope Analysis (SEA) [18, 22].

Mathematically, the raw signal generated by a defect (e.g., a defect on the ring raceway) is expressed as a sum of amplitude-modulated impulse responses:

$$\mathbf{u(t) = \sum_{k=-\infty}^{\infty} A_k \cdot s(t - kT - \tau_k) + n(t)} \qquad (1)$$

Where $A_k$ represent the amplitude modulation and represents the variation of the impact force. As the defect passes through the bearing loading zone, the shock amplitude increases and decreases:

$$\boldsymbol{A_k = A_0[1 + m \cdot \cos(\omega(t))]} \qquad (2)$$

The $\omega(t)$ represents the angular speed expressed by:

$$\boldsymbol{\omega(t) = 2\pi f} \qquad (3)$$

Where $f$ represents the shaft speed.

Another component of the expression is the impulse response (or carrier signal), noted with $s(t)$ is the transient vibration of the machine structure excited by the fault shock. It is discribed as a damped sinusoid:

$$\boldsymbol{s(t) = e^{-\alpha t} \cos(2\pi f_r(t) + \varphi))} \qquad (4)$$

With $f_r$ - resonance frequency and $\alpha$ - damping coefficient. The impact periodicity represents the theoretical interval between two impacts and is described by $kT$. In expression 1 a random variable

 doi:10.20944/preprints202604.1651.v1



($\tau_k$) that describes the small time variations caused by the slippage of the rolling elements, which makes the signal cycle-stationary, not perfectly periodic. The background noise coming from other components, motors, slides, pumps, cooling system, tool change and measurement errors are expressed by the parameter *n(t).* To isolate the defect from the background noise n(t) the Hilbert Transform is applied to a specific frequency domain, using a bandpass filter method. To isolate the defect from the background noise *n(t)* the Hilbert Transform is applied to a specific frequency domain, using a band-pass filter method [22, 23]. The choice of the filter band is the critical step, because that is where the structural resonance specific to the bearing elements is located, being excited by the shock. One of the most useful band-pass filtering methods is a mathematical method based on the Kurtosis method, determining the degree of impulsivity for different frequency bands. The mathematical expression of spectral Kurtosis *K(f)* for a frequency-centred band is:

$$\mathbf{K(f)} = \frac{\langle |\mathbf{X(t,f)}|^4 \rangle}{\langle |\mathbf{X(t,f)}|^2 \rangle^2} - \mathbf{2} \tag{5}$$

where *X(t,f)* is the time-frequency representation of the signal. The frequency band where *K(f)* has the maximum value is chosen. A high Kurtosis indicates the presence of repetitive shocks (the defect), while a Kurtosis close to 0 indicates Gaussian noise (without defect). Once the optimal filter band is identified a band-pass filter $H_{bp}(f)$ is applied, the filter range depends on the spindle type.

$$\mathbf{u_f(t)} = \mathbf{F^{-1}}\left[\mathbf{X(f)} \cdot \mathbf{H_{bp}(f)}\right] \tag{6}$$

The Hilbert transform is a linear operator that shifts all spectral components of a signal by -90° or (-π/2). Mathematically, for a real signal *u(t),* the Hilbert transform $\hat{\boldsymbol{u}}(\boldsymbol{t})$ is defined by convolving the signal with the function (1/πt):

$$\hat{\boldsymbol{u}}(\boldsymbol{t}) = \boldsymbol{H}[\boldsymbol{u}(\boldsymbol{t})] = \frac{\mathbf{1}}{\boldsymbol{\pi}} \int_{-\infty}^{\infty} \frac{\boldsymbol{u}(\boldsymbol{\tau})}{\boldsymbol{t}-\boldsymbol{\tau}} \boldsymbol{d\tau} \tag{7}$$

Then, the Synchonous Envelope Vibration Analysis method in both the time and frequency domains is used to identify the critical impact frequencies of the bearing spindle [18, 22]. Moreover, the harmonics and interharmonics are highlighted to determine their distribution and repeatability.

During machining processes, spindles can determine a new optimized set of machining parameters, allowing for self-optimization of condition monitoring and control of the machining process. Autonomy is also reflected in the self-diagnosis and self-assessment of spindle health. Smart spindle should be able to assess their current state of degradation, so that the operating status of the shaft can be transmitted back to the machine controller, allowing for real-time maintenance of operations to avoid potential problems and thus ensure preventive maintenance. In this context, an AI-based model is proposed starting from the monitoring model based on the vibration synchrony determination method, presented in the figure 3.

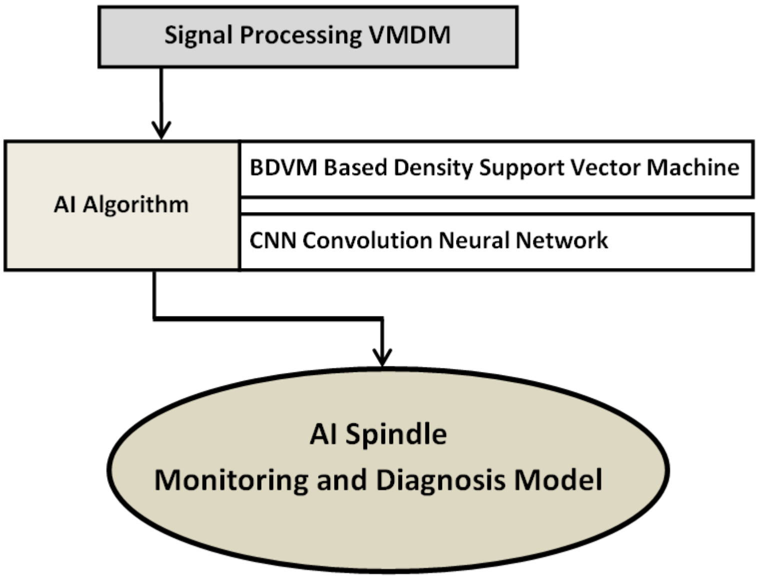

 doi:10.20944/preprints202604.1651.v1



**Figure 3.** The proposed Monitoring Diagnosis Model, MDM.

The Base Density of the Support Vector for Machine Learning (BDSVM) has been beneficial in establishing the basic data for neural network learning. In any monitoring activity, it is more efficient to train the neural network using BDSVM, as it reduces the learning input data (decreasing computational complexity) and determines the resulting weight matrices to identify mechanical failure without being affected by outliers.

The architecture of the intelligent monitoring system is shown in Figure 3, where the data collection and data processing steps are included. In this system, machine learning algorithms are adopted for improving the performance of fault detection in the intelligent monitoring system.

For researchers to determine the characteristic frequencies of faults, conventional spindle monitoring requires accurate bearing information, including the diameter of balls, pitch diameter, contact angle, and number of rolling elements. However, feature design expertise is required for manual feature design, and bearing information is rarely available for legacy machines or for specialized equipment. Through autonomous feature learning, deep learning provides a customized method to solve this problem, using convolutional neural networks for learning features from vibration data. The CNN learns hierarchical features in which lower layers detect basic trends, middle layers generate fault signals, and signals are projected into health states by upper layers. With respect to the implementation of Industry 4.0, the requirement-free approach has significant advantages, such as scalability across different machine fleets, the ability to modify already installed machines with unknown specifications, reduced engineering effort, and simplicity for operators who are not specialized. With respect to the comparison with the simple metric methods, the multi-sensor fusion has the advantages of increasing the reliability of diagnosis automatically by using developed calculated combinations. Three complementary vibration metrics form the foundation of our approach. Radial velocity (mm/s) represents the RMS velocity following ISO 10816 standards, calculated as

$$\mathrm{v_{RMS}} = \sqrt{\frac{1}{\mathrm{T}}\int_0^{\mathrm{T}} \mathrm{v(t)^2 dt}} \qquad (8)$$

Where $v$(t) is the instantaneous velocity, and $T$ is the signal duration and is sensitive to low-frequency faults. The envelope acceleration, $gE$, is a feature that uses high frequency demodulation, specifically for bearing fault detection, and is calculated through band-pass filtering, Hilbert transform, and RMS computation to identify impulse signals caused by bearing faults, which can provide 3-6 months' warning time instead of velocity measurements. Broadband radial acceleration, g, is used to assess the condition and covers the range of low and high frequencies. All the attributes are then normalized using Min-Max normalization, where the result is calculated as follows:

$$x_{norm} = \frac{x - x_{min}}{x_{max} - x_{min}} \qquad (9)$$

to ensure equal contribution during training. The neural network outputs a continuous health score

$$H(v) = e^{-\alpha v} \quad H \in [0,1] \qquad (10)$$

where values above 0.7 indicate fair condition (Healthy: H > 0.7), 0.3-0.7 (Warning: $0.3 \leq H \leq 0.7$) represent a warning requiring action, and below 0.3 (Critical: H < 0.3) indicate critical condition requiring immediate action. The spindle should have the ability to update its performance through self-learning. In general, cutting conditions vary frequently, and the smart spindle should analyze and learn from these cases, so that a self-evolution strategy can be implemented by using self-learning algorithms. With the support of databases and base knowledge, smart spindle can discover new knowledge from field data, without the guidance of operators, continuously improving their performance and level of intelligence. An intelligent spindle should have high autonomy to perform its functions efficiently. For example, in the preparation stage, before machining using the spindle, measures are needed to automatically minimize setup time (e.g., precision balancing time) and to automatically select process parameters (e.g., feed rates, depth of cut, spindle speed) to achieve target quality, productivity, and efficiency requirements. In the case of the spindle, the main element that can be controlled, adapted and adjusted is the speed, so that it is able to overcome critical operating areas or even automatic limitation. In this paper, such a model is proposed that, in addition to determining the operating state in real time, can also adapt in the operating loop so that it can avoid or limit certain operating areas (figure 4).

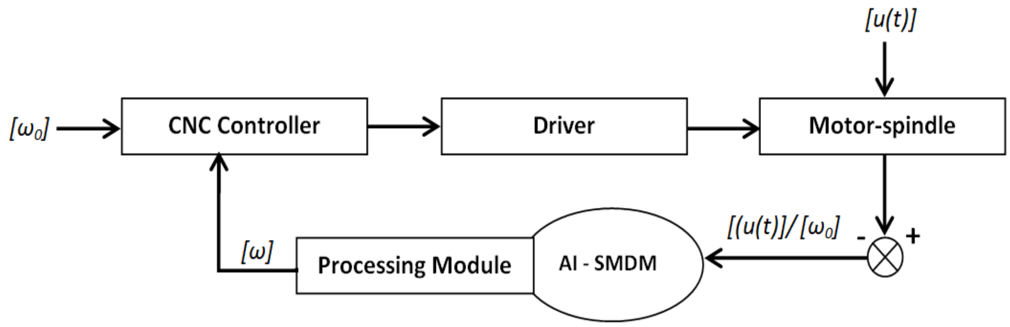


**Figure 4.** Operation loop with AI SMDM model integration.

## 3. The Experimental Setup

The research work was developed with the aim of intelligent monitoring of the motor-spindle in high-speed milling machine tools. The method is based on the determination of the Fourier acceleration spectra and the Hilbert transforms of these spectra, in order to determine the evolution of wear in the main shaft bearings. Thus, the increase in the amplitude of the vibrations in the Fourier spectrum, specific to the bearings, is highlighted with the determination of the envelope of these spectra. The method of calibrating the permissible wear limit of the bearings, up to which the main shaft can be used, and respectively the highlighting of the evolving spectra, as well as the Fourier spectra after replacing the worn bearings, was highlighted. The determinations were carried out on an experimental stand that includes a high-speed center milling machine, accelerometers for each axis as well as a laser sensor for determining the speed.

### *3.1. Description of the Setup*

The experimental set-up is an industrial application thats highlights the condition of a motor spindle of a milling center machine type Doosan NX 5500, with a 50HSK tool holder, 22kW spindle power and 20000 RPM rotational speed.

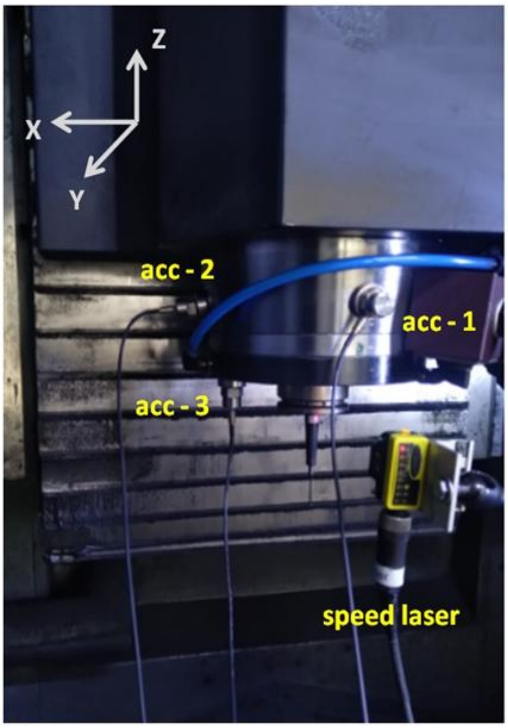



a b

**Figure 5.** The used experimental set-up.

Vibrations are measured by three accelerometers fixed in the x, y and z directions of the spindle. While synchronization with the speed is achieved by means of a laser speed sensor (figure 5a). The experimental data are collected by using the acquisition board type National Instrumens USB4431 and with the specific Fastview software with a new application Spindleview, fig.5b.

### *3.2. Research Method and Some Results*

The application is a high-speed motor spindle with intelligent vibration monitoring and control functions, which includes three modules: detection (real-time condition monitoring), decision-making (vibration prediction), and control (active critical speed control). The detection module includes sensors that are used or integrated into the spindle structure to measure the vibration signals of the spindle housing, tool holder and thermocouples that are used to measure the temperature at the motor and at the bearings. Temperature measurement is crucial but bearing failure is revealed at an early stage by vibrations. Synchronizing vibrations with temperature is the key to monitoring and diagnosing high-speed spindles, figure 3 [18]. When in addition to the existence of critical vibration parameters there is also an increased thermal evolution, the level of wear is very advanced.

 doi:10.20944/preprints202604.1651.v1



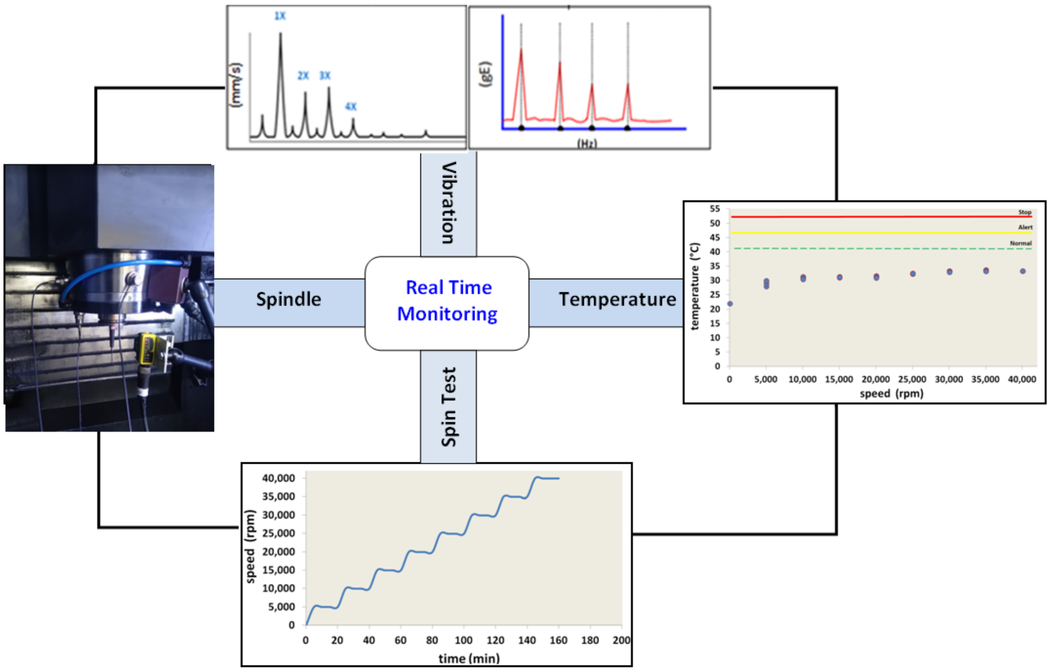


**Figure 6.** Spin test parameters in real-time monitoring condition of motor-spindle.

The used algorithm presented in figure 2 shows the procedure of collection, processing, filtration, calculation under stable temperature conditions. Thermal effects are indispensable in monitoring and must be taken into account at all times. When the spindle reaches the alert limit, the specific diagnosis is focused not only on vibrations but also on the heat source. Finally, with the collected experimental data, the Fourier spectra were determined, and by applying the Hilbert transform, the enveloped acceleration spectra were obtained, according to the procedure in figure 2. By using these characteristics will be possible to see the tendences of the bearing defect and the limit of acceptance. Considering the type of bearings specific to spindles, the essential component is in the radial, x or y direction, shown in the figure 7. The first monitored and measured characteristic is acceleration, being crucial in making a decision, both as a measurement and filtering domain and as a diagnostic domain. Figure 7 presents the acceleration frequency spectra, at a speed of 10,000 rpm, for 4 different dates, 23 May (a), 7 July (b), 30 October (c) and 19 December (d), as well as the acceleration spectrum for the situation after repair (e), as a healthy state of the spindle

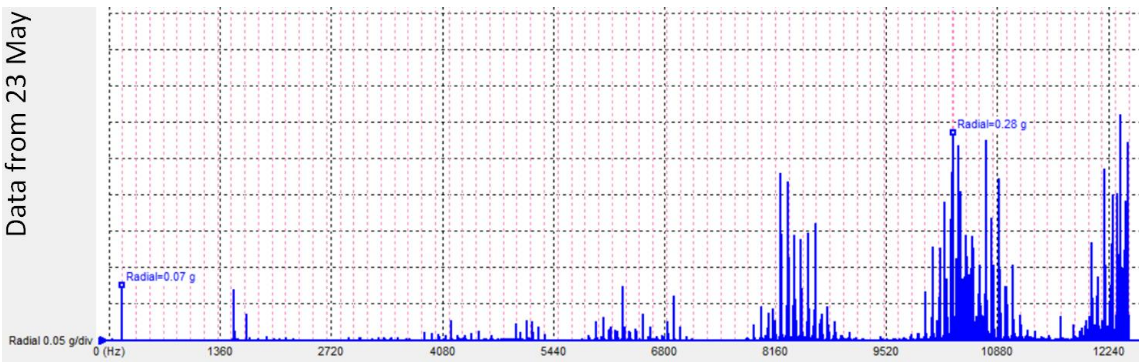


a- Accelreation RMS from 23 May

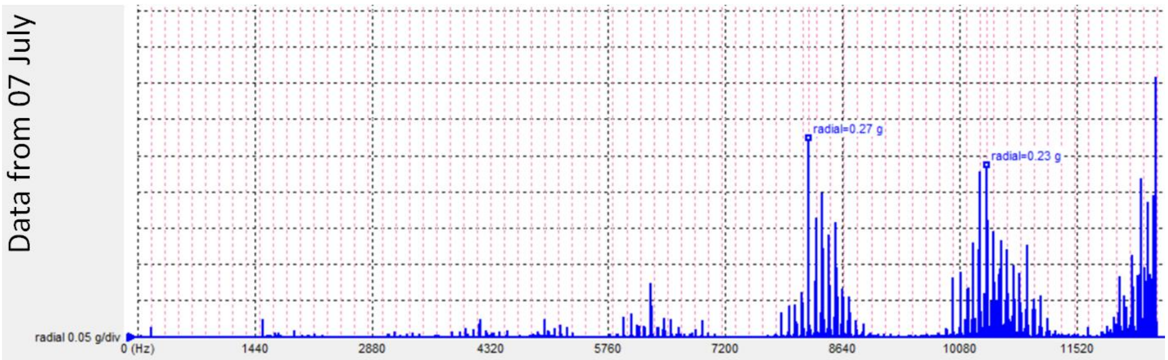


b- Accelreation RMS from 07 July

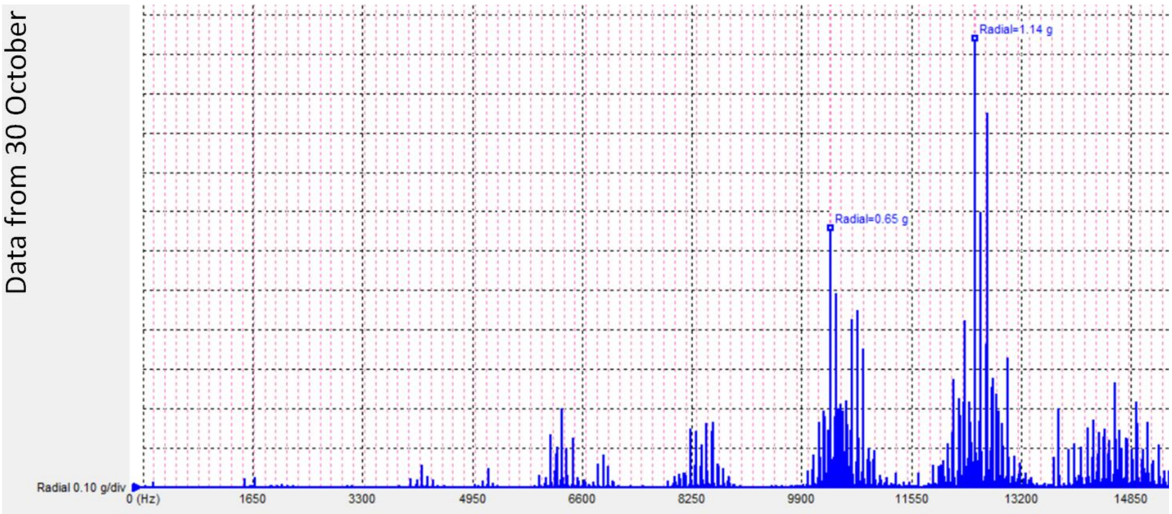


c- Accelreation RMS from 30 October

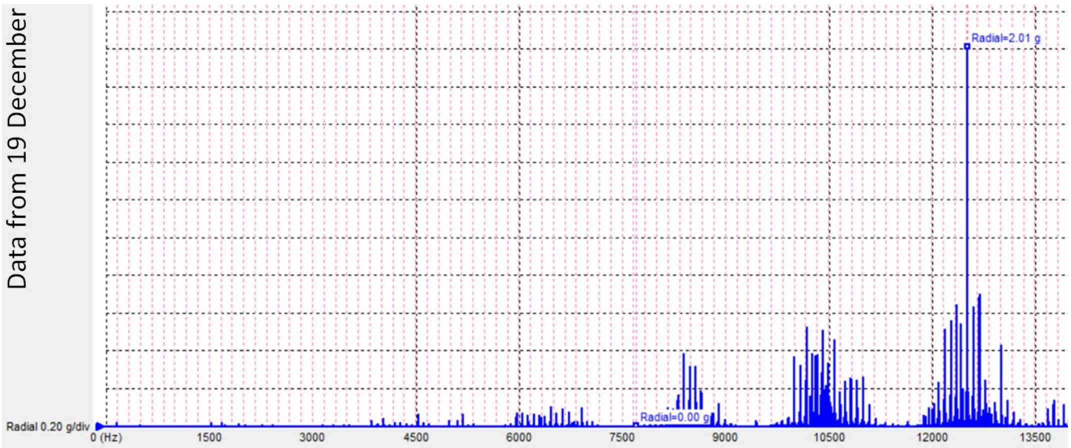


d- Accelreation RMS from 19 December

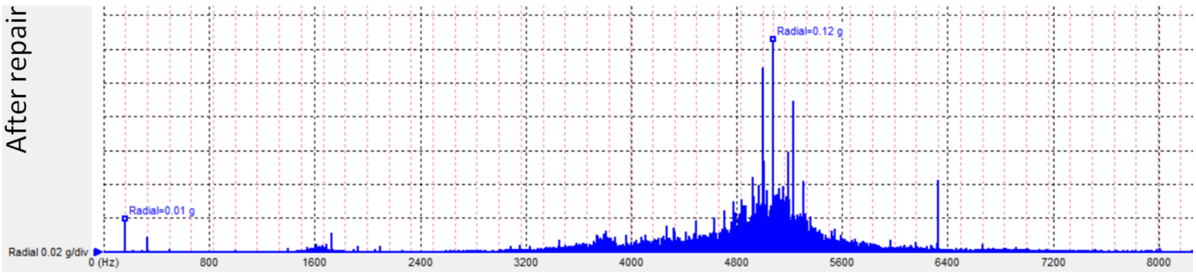

e- Accelreation RMS after reapir (new status)

**Figure 7.** Monitoring of the acceleration Fourier spectra of the spindle.

The Hilbert transform (HT) is an integral transform that plays a significant role in vibration signal processing. There are two ways it can be used. First, HT provides a direct examination of the instantaneous attributes of a vibration: frequency, phase, and amplitude. It also allows the analysis of quite complex systems in the domain of time. Second, HT is used to find the real part of the transfer function of a system separated from the imaginary part of the system and vice versa. This allows systems to be analyzed in the frequency domain. HT can be used as an intermediate step in the more elaborate analysis of a system. In addition to analyzing the transfer function as a frequency response, it is useful for hysteretic damping characterization and nonlinear system identification [23]. The research aims to identify the operating state in real time by complexly approaching the monitored signals both in the low frequency domain (imbalance, mechanical weaknesses, resonance, poor lubrication, electrical problems, etc.) and in the high frequency domain (bearings, converter frequencies, etc.). The model presents the ability to evaluate the fault state by monitoring both the vibration level as the ISO limit (ISO21940, ISO20816) or predefined threshold for gE acceleration and the sidebands related to the fault frequencies. The vibrations caused by various faults and their combinations are analyzed and assigned to fault typologies synchronized with the specific frequencies, thus being used to train ANN-based machine learning, like BDSVM and CNN.

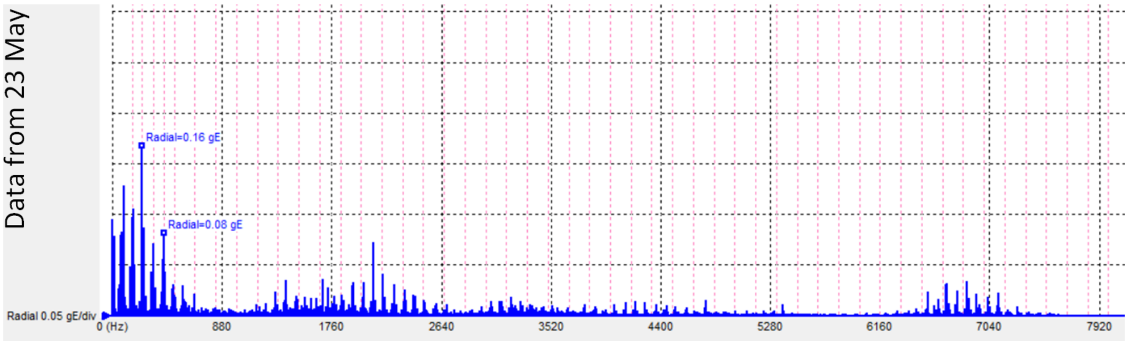


a- Acceleration envelope from 30 May

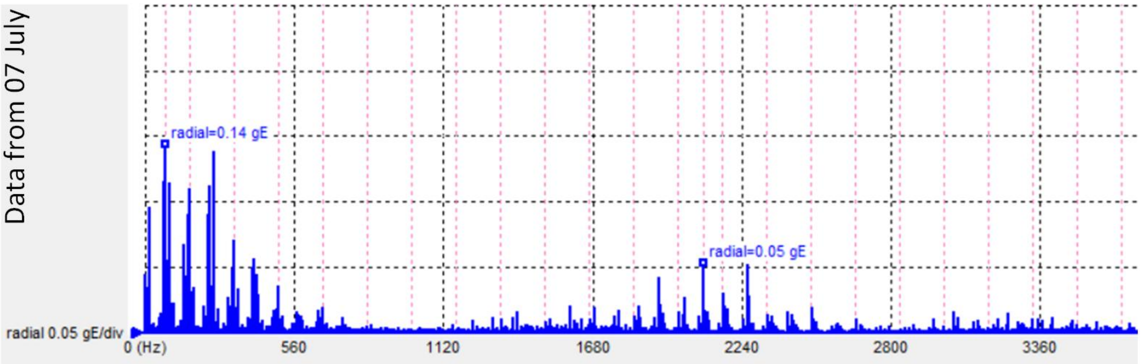


b- Acceleration envelope from 07 July

 doi:10.20944/preprints202604.1651.v1



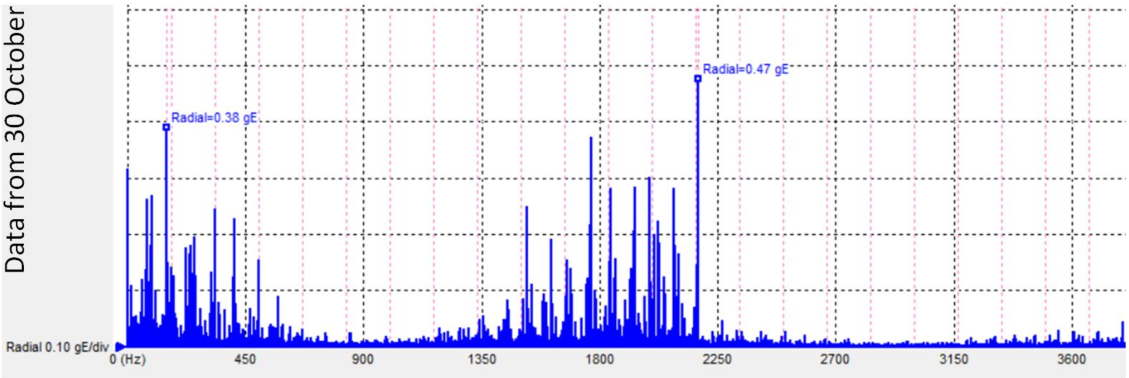


c- Acceleration envelope from 30 October

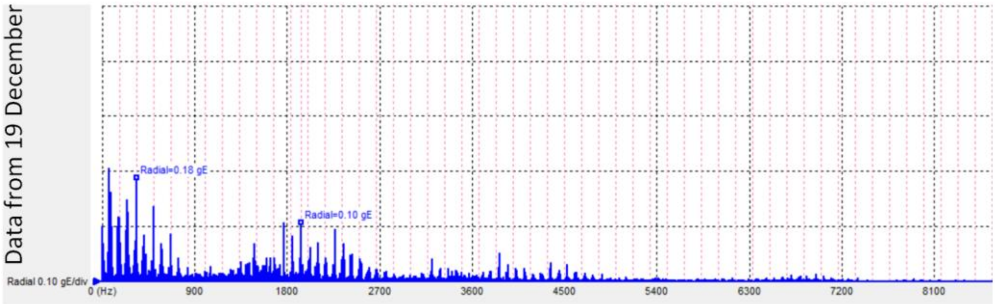


d- Acceleration envelope from 19 December

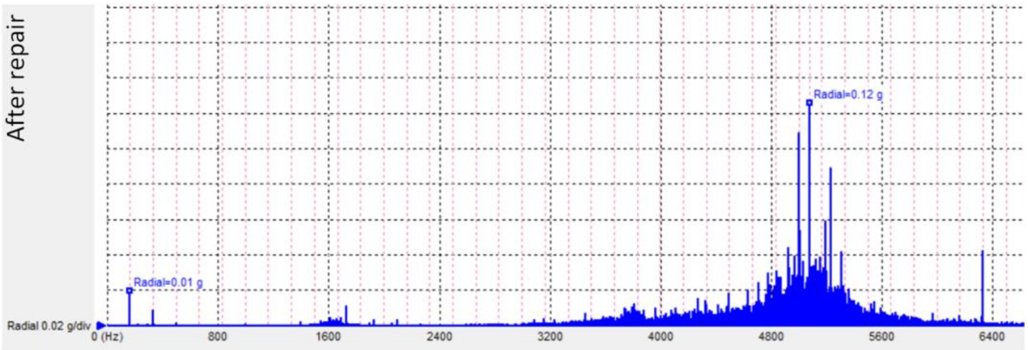


e- Acceleration envelope after repair.

**Figure 8.** Acceleration envelope after applied the Hilbert Transform.

Figure 8 shows the frequency spectra related to the enveloped acceleration according to the method presented in section 2, at a speed of 10,000 rpm. Based on the collected data, acceleration and envelope acceleration, the proposed AI methods are applied. The first method is DBSVM designed to more efficiently handle data sets where the distribution of points is not uniform [24]. In the case of spinels, DBSVM can identify areas with high density of normal operation and can signal subtle deviations that precede a failure.

### *3.3. The Optimisation Function*

The optimization function (*OF*) was proposed as a polynomial function of the fifth order with real coefficients that will be constructed by using the data from the acquisition of Fourier spectrum of the vibrations:

$$FO = a_1x^5 + a_2x^4 + a_3x^3 + a_4x^2 + a_5x + a_6 \quad (11)$$

where $a_i$ will be determined by using the matrix equation

Preprints.org (www.preprints.org) | NOT PEER-REVIEWED | Posted: 23 April 2026 doi:10.20944/preprints202604.1651.v1



$$\begin{pmatrix} a_1 \\ a_2 \\ \cdots \\ a_6 \end{pmatrix} = \left\{ \begin{bmatrix} x_1^5 & \cdots & x_1 & 1 \\ \vdots & \ddots & \vdots & \\ x_5^5 & \cdots & x_5 & 1 \end{bmatrix} \begin{bmatrix} x_1^5 & \cdots & x_1 & 1 \\ \vdots & \ddots & \vdots & \\ x_5^5 & \cdots & x_5 & 1 \end{bmatrix}^T \right\}^{-1} \begin{pmatrix} FO_1 \\ \cdots \\ FO_5 \end{pmatrix} \qquad (12)$$

with the following constraints:

- *$x_i$>0;*
- *$x_i$ must be meaningful points, $x_i \in$ group 1;*
- *$x_i \in$ BDSVM,*

where *$FO_i$* is the amplitude of the vibration evolution in time where the defect will appear and $x_i$ is the frequency. To define the *OF*, 5 boundary points ($x_i$, $FO_i$)∈*BDSVM* will be used for each moment of time vs. frequency points but under the same conditions of forced vibration and for the same milling machine. The Based Density Suport Vector Machine points must strictly adhere to the condition of belonging to BDSVM which is that:

*$d_i$ <average_d* . (13)

where $d_i$ is the distance between the points and $d$ is the average of these distances.

*If $d_i$ >d,*
*the point i is in the outlier group;*
*Else*
*the point i will be considered important (meaningful) points in BDSVM;*
*End.*

This study exploits this method to find the most relevant data points and establish the objective function (*OF*) [27].

### *3.4. The used LabView Software and the Obtained Objective Function*

The LabView virtual instruments were developed with the aim of generating objective functions specific to the vibrational behavior of the main shafts in the high-speed milling machine. The objective functions of the 5th order polynomial type were generated and the coefficients of these functions were determined. The characteristics of the objective functions were drawn in various data in order to monitor the evolution of defects in the bearings of the main shaft as well as to determine the wear tendency and the establishment of the acceptable limit of wear. The virtual LabView instrumentation were shown in the figures 9-13. The objective function for the different time of the data acquisition were descibed in the relations (4).

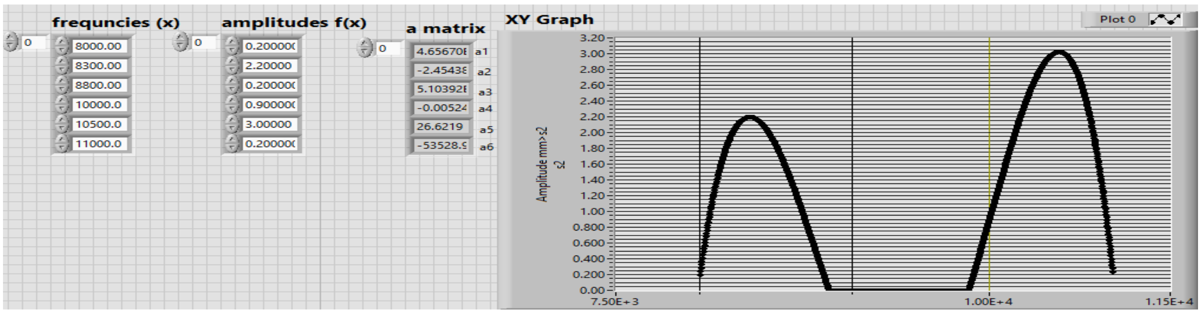


**Figure 9.** Front panel of the LabView virtual proper instrument.

We can see the input data chosen by using the properties of the BDSVM between the all acqusition data, frequencies vs.amplitude of the vibration in part of *g*.

Preprints.org (www.preprints.org) | NOT PEER-REVIEWED | Posted: 23 April 2026 doi:10.20944/preprints202604.1651.v1



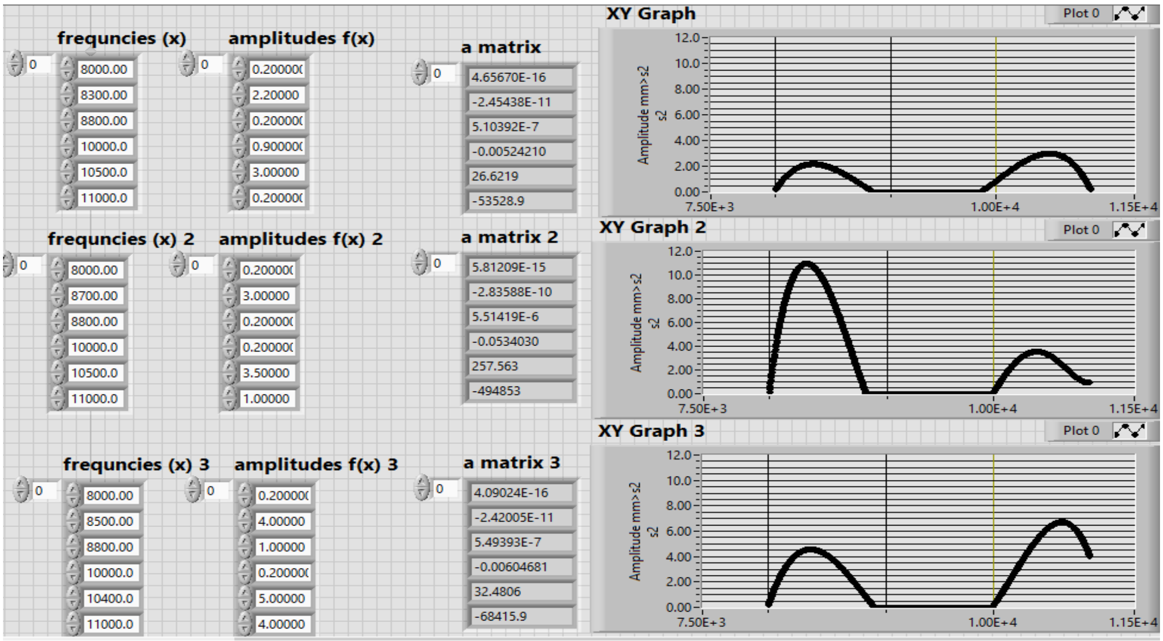


**Figure 10.** Tendences of the obiective functions (*OF*) in different time of wear evolution.

$$FO = (4.65\mathrm{E}-16)x^5 - (2.45\mathrm{E}-11)x^4 + (5.103\mathrm{E}-7)x^3 - 0.0052x^2 + 26.6219x - 53528.9 \tag{14}$$

$$FO = (5.81\mathrm{E}-15)x^5 - (2.835\mathrm{E}-10)x^4 + (5.514\mathrm{E}-6)x^3 - 0.0534x^2 + 257.563x - 494853 \tag{15}$$

$$FO = (4.09\mathrm{E}-16)x^5 - (2.42\mathrm{E}-11)x^4 + (5.493\mathrm{E}-7)x^3 - 0.006x^2 + 32.4806x - 68415.9 \tag{16}$$

Where $FO_i$ are the amplitude of the vibration and $x_i$ are the frequencies.

The amplitude of the vibration must respect the the following constrait:

*If FO<0.0 then*

*FO=0.0*

*Else*

*FO=FO;*

*End.*

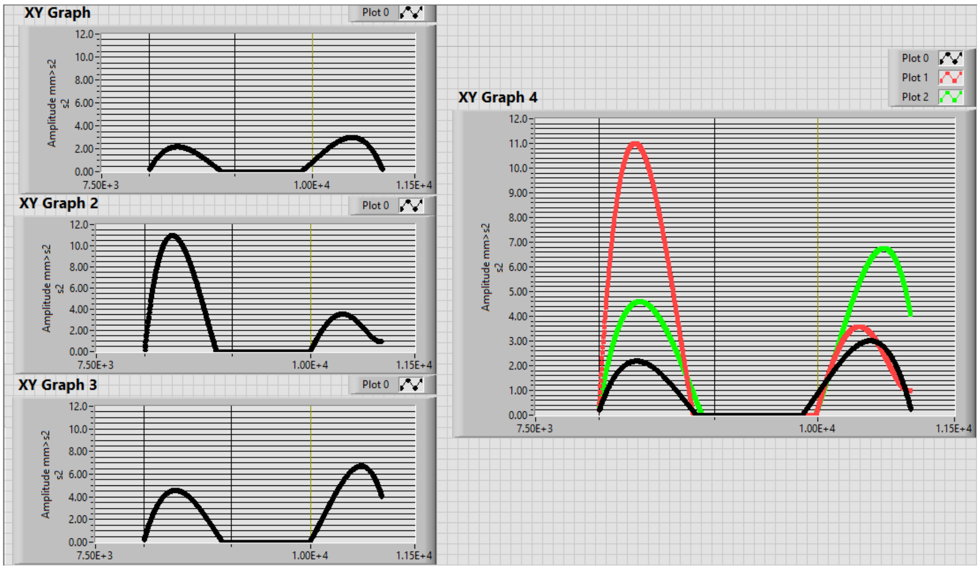


**Figure 11.** The comparative characteristics in different time of evolution.

 doi:10.20944/preprints202604.1651.v1



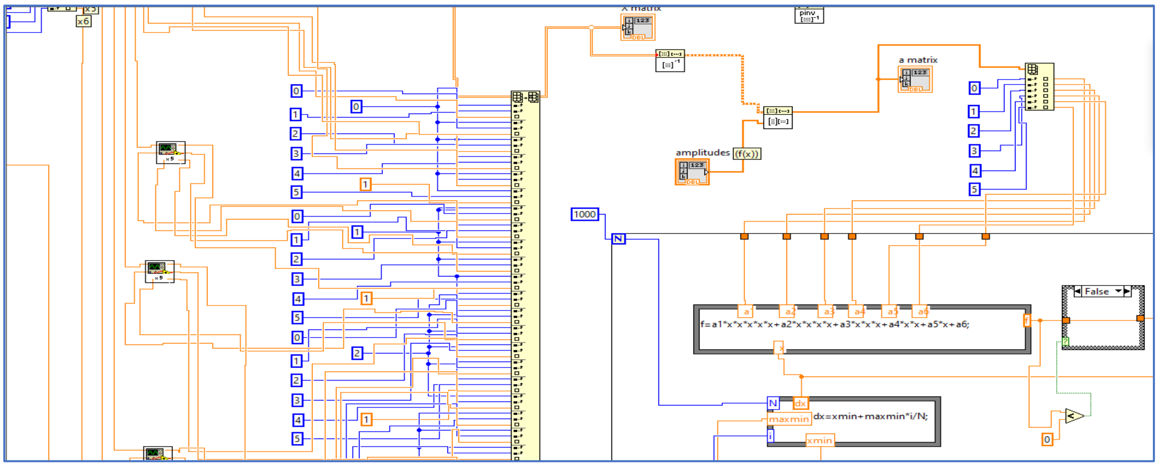


**Figure 12.** Part of the LabView block diagrame of the obiective function.

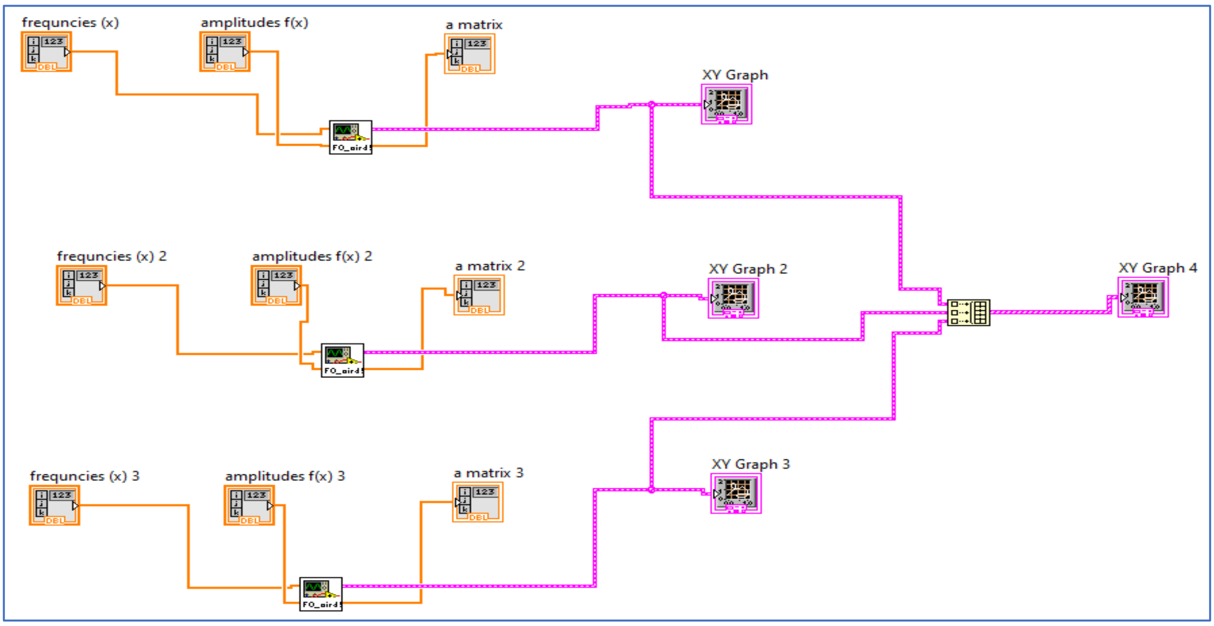


**Figure 13.** Block diagram of the LabView proper virtual instrument for the comparative characteristics for different time of wear evolution.

*3.4. Deep Learning Based spindle Vibration Analysis and Control*

In this stage, I propose to develop the theoretical framework used to predict bearing fault frequencies. The proposed plan includes:

- Deriving fundamental bearing fault frequencies like (BPFI -Ball Pass Frequency Inner rase, BPFO- Ball Pass Frequency Outer rase, BSF- Ball Spin Frequency, and FTF- Fundamental Train Frequency) from first principles;
- Identifying the dominant excitation sources like unbalancing, misalignment, bearing defects, and cutting-induced vibrations;
- Predicting the critical frequency bands that may contribute to instability or chatter.

These insights are used to benchmark the experimental data collected on vibration response, and they serve as the basis for designing learning-based vibration control strategies.

The outer and inner race frequencies of the bearing are calculated with the following relations:

$$BPFO = \frac{n}{2} f_r \left(1 - \frac{B_d}{P_d} \cos\theta\right) \tag{17}$$

$$BPFO = \frac{n}{2} f_r \left(1 + \frac{B_d}{P_d} \cos\theta\right) \tag{18}$$

 doi:10.20944/preprints202604.1651.v1



where: n- number of the rolling elements; $B_d$ – ball diameter; $P_d$ – pitch diameter; $\theta$- contact angle; *RPM*- shaft speed; $f_r$ -rotational frequency.

The second ANN used is CNN method, an AI architecture specialized in data processing using convolutional datasets to automatically learn feature hierarchies. In the case of spindles, especially since they operate at variable speeds, the CNN can be trained to recognize the defect regardless of the rotation speed

*3.5. The CNN Convolutional Neural Network for Spindles*

We chose a one-dimensional Convolutional Neural Network model, specifically designed for time series analysis of the data on the machine's vibration. The choice of this model is justified for three main reasons: pattern recognition for identifying fault signatures regardless of their location on the machine, feature learning for recognizing simple patterns and gradually moving on to more complex fault signatures, and the efficiency of the model's parameters for preventing overfitting due to the small dataset (89 data measurements). The model's structure is composed of an input layer for inputting the data, with the sequence length being 10 and the number of features being 3, followed by two convolutional layers with 64 and 32 filters and a kernel size of 3, ReLU activation function, batch normalization, and pooling; a flattening layer; and two dense layers with 64 and 32 units, and a softmax layer with 4 units for classification. The total number of parameters is around 45,000, much less than that of a fully connected network.

$$\hat{y}\_k = \frac{e^{z\_k}}{\sum_{j=1}^{4} e^{z\_j}} \tag{19}$$

The pyramid filter structure of 64→32 supports hierarchical learning, in which earlier layers learn varied low-level patterns, with later layers combining these into higher-level features. The kernel size of 3 supports local temporal dependencies in a computationally efficient manner. Dropout values of 20-30% avoid overfitting while retaining learning ability, and batch normalization improves training stability, reducing training time by 40%. Training used categorical cross-entropy loss

$$L = -\sum_{i=1}^{4} y\_i \log \hat{y}\_i \tag{20}$$

with Adam optimizer and learning rate 0.001, and data augmentation using Gaussian noise, time shifting, and amplitude scaling. This setup resulted in 96% accuracy, which was better than SVM (85%) and Random Forest (89%) classifiers.

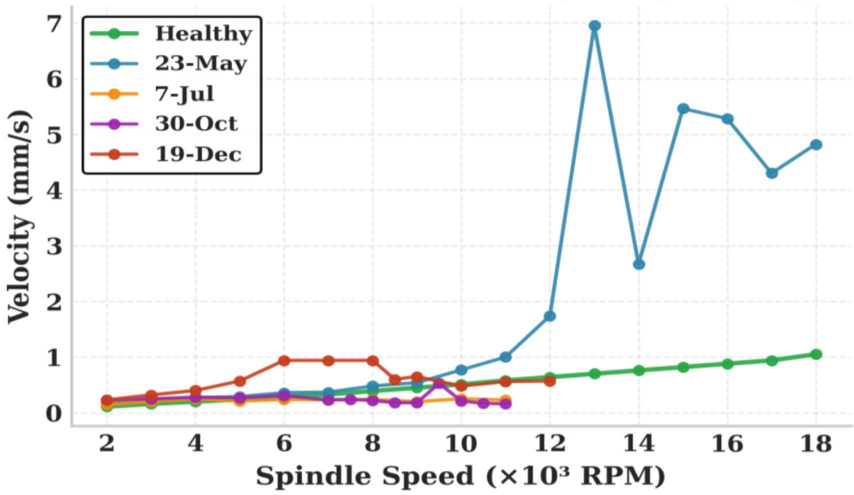


**Figure 14.** Initial data set: velocity vibration.

 doi:10.20944/preprints202604.1651.v1



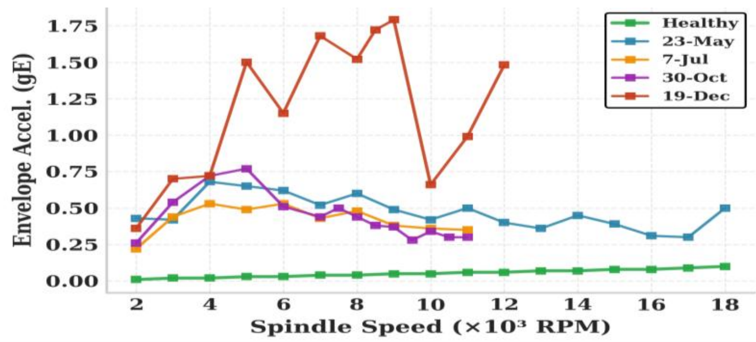


**Figure 15.** Initial data set: envelope acceleration.

The experimental data cover a spindle speed range from 2,000 to 20,000 RPM. Machine condition is evaluated using three vibration metrics: broadband radial acceleration (g) for overall condition assessment, envelope acceleration (gE) for bearing fault detection, and derived radial velocity (mm/s) in accordance with ISO 10816 for severity comparison. Radial velocity was obtained from the measured acceleration signals using standard signal processing procedures.

Measurements were conducted over seven months and represent different stages of machine health.

The healthy data set has 19 measurements within the 2,000-20,000 RPM range. Both acceleration- and velocity based indicators are at low levels over the entire operating regime. The radial velocity, as calculated, increases steadily with operating speed but at levels below 1.1 mm/s, thus confirming normal operating conditions in accordance with ISO 10816.

The 23-May data set indicates the beginning of a degradation process. Seventeen measurements were recorded over the 2,000-18,000 RPM operating regime. Compared with the healthy condition, a moderate increase in vibration levels is detected. Radial velocity has a steady increase with operating speed, with levels near 1.0 mm/s, while broadband acceleration and envelope acceleration also show corresponding increases, reflecting the beginning of bearing degradation.

The 7-July dataset is related to a progressive degradation stage, with 15 measurements recorded in the 2,000-16,000 RPM range. Both velocity and acceleration levels are increased in comparison to the early degradation stage. Radial velocity levels exceed 1.5 mm/s at increased speeds, with high levels of broadband and envelope acceleration, thus confirming the progression of the fault.

The 30-October dataset relates to an advanced degradation stage, with 14 measurements recorded in the 7,500-10,500 RPM range. Velocity levels are high but stable over the entire recorded range, while acceleration-based indicators show high levels, thus confirming a developed fault with limited growth.

This dataset is for the 19-Dec condition, which is for the critical stage of degradation with 12 measurements. There are highly increased levels of vibration, with broadbands of radial acceleration greater than 6.5 g and up to 1.8 gE, which is near failure.

For the main part of the paper, the following datasets are chosen: healthy, 23-May (early degradation), 30-Oct (advanced degradation), and 19-Dec (critical degradation). These datasets clearly indicate the development of machine degradation over time and allow us to find the critical point, or “knee point,” in the machine's vibration response. The 7-Jul progressive degradation dataset and the after repair dataset, which confirms the success of the repair, are presented in the supplementary material.

## 4. Results and Discussion

The Base Density Support Vector Machine (BDSVM) plays an important role in gathering the vibrational data earlier than the deep learning analysis. It is different from other conventional methods, which consider all data points equally. It will identify the dense regions that correspond to the normal conditions and firstly represent operating conditions, while filtering out sparse, isolated points that correspond to noise or non-representative events. This is the important thing in the spindle monitoring, where the data distribution is non-uniform due to variations of rotational speeds,

 doi:10.20944/preprints202604.1651.v1



load conditions, and transient effects.

The integration of BDVSM with the CNN model results in an efficient diagnostic pipeline. In this manner, BDSVM is used as a preprocessing stage, and it reduces the dimensions and improves the quality of the input dataset. The CNN model operated on the refined dataset to learn hierarchical fault features, and it classifies the spindle health state. The convergence between these two methods improves robustness and accuracy.

In place of implementing either approach separately, the system as a whole achieved greater stability. From a physics point of view, the BDVSM method perfectly fits the characteristics of spindle vibration data. In real conditions, mainly in industries, most of the operating states form dense clusters corresponding to the stable machine behavior, while the faults deviate from these clusters.

Figure 16 illustrates the progression of the health scores using the neural network approach at four stages of monitoring (23-May, 7-Jul, 30-Oct, and 19-Dec). During the May monitoring, the health scores are high at low and medium spindle speeds but drop sharply at speeds above 9,000 RPM, going below the early warning level (0.8) and indicating impending failure at high-speed usage. During the July monitoring, the health scores are relatively stable at all speeds, though a steady deterioration with increasing RPM is still observed, as expected for progressive degradation.

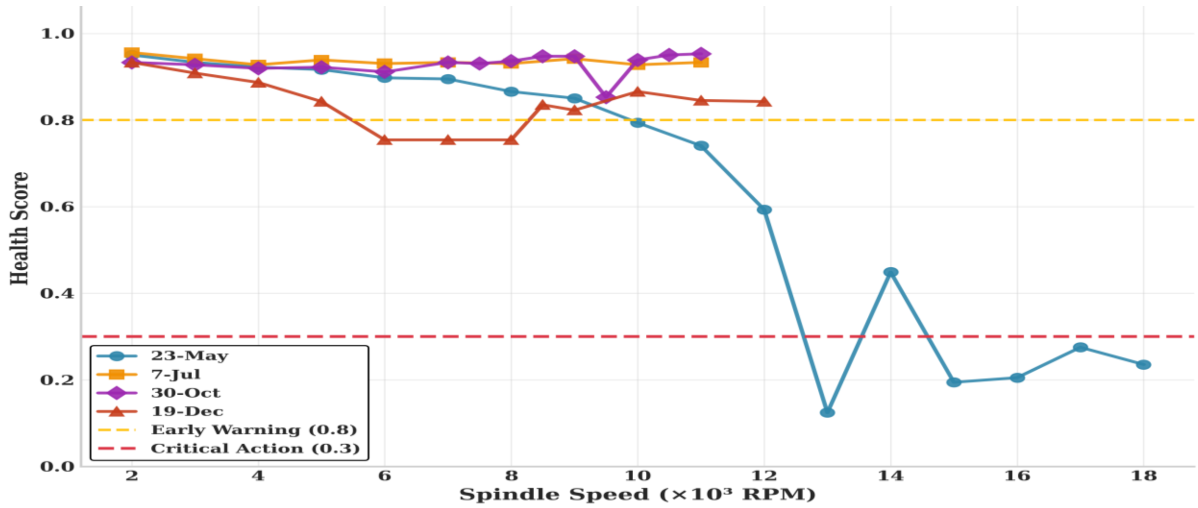


**Figure 16.** Neural Network Health Score Projection Result.

During the October monitoring, the health scores are relatively uniform and high, staying well above the critical level, which indicates a brief point of stability in the system condition. Conversely, during the December monitoring, the health scores are steadily decreasing, especially at higher speeds, indicating a state of advanced degradation and susceptibility to failure.

Preprints.org (www.preprints.org) | NOT PEER-REVIEWED | Posted: 23 April 2026 doi:10.20944/preprints202604.1651.v1



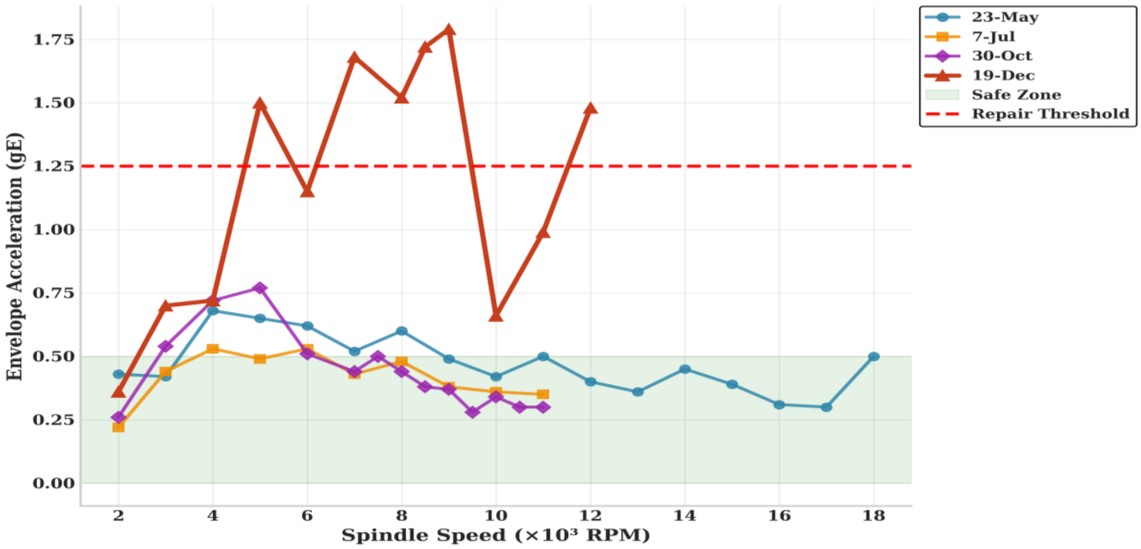


**Figure 17.** Repair thresholds.

As illustrated in Figure 17, the envelope acceleration analysis represents a highly sensitive fault detection measure for rolling bearings. Envelope acceleration emphasizes high-frequency impact components generated by localized bearing defects, which are typically attenuated in velocity-based measurements.

According to the degradation data, three reference thresholds are established: a warning threshold of 0.50 gE, indicating early-stage fault detection and requiring inspections within 1-2 months; a critical threshold of 1.00 gE, indicating late-stage fault detection and requiring maintenance within 1-2 weeks; and a repair threshold of 1.25 gE, represented by a red dashed line, indicating a high risk of catastrophic failure and requiring immediate action. These reference thresholds are based on ISO 10816 vibration severity guidelines.

In the 23-May measurement data, it can be seen that the envelope acceleration level is still below the warning threshold for most of the operating speeds, thus supporting the decision that a routine inspection is appropriate. In the 7-Jul measurement data, however, it can be seen that the vibration level is approaching the warning threshold as the spindle speeds are higher, thus indicating early-stage defects. In the 30-Oct measurement data, it can be seen that the vibration level is approaching and even exceeding the warning threshold.

In 19-Dec, the most severe condition is observed, as indicated by the measurements, where several operating speeds are above the critical level, and several measurements are above the repair level. This indicates that urgent attention is required for bearing replacement. In addition, significant variations are observed, indicating that resonance and fault mechanisms, such as bearing damage and secondary imbalance, associated with unstable operation and failure are occurring.

Preprints.org (www.preprints.org) | NOT PEER-REVIEWED | Posted: 23 April 2026 doi:10.20944/preprints202604.1651.v1



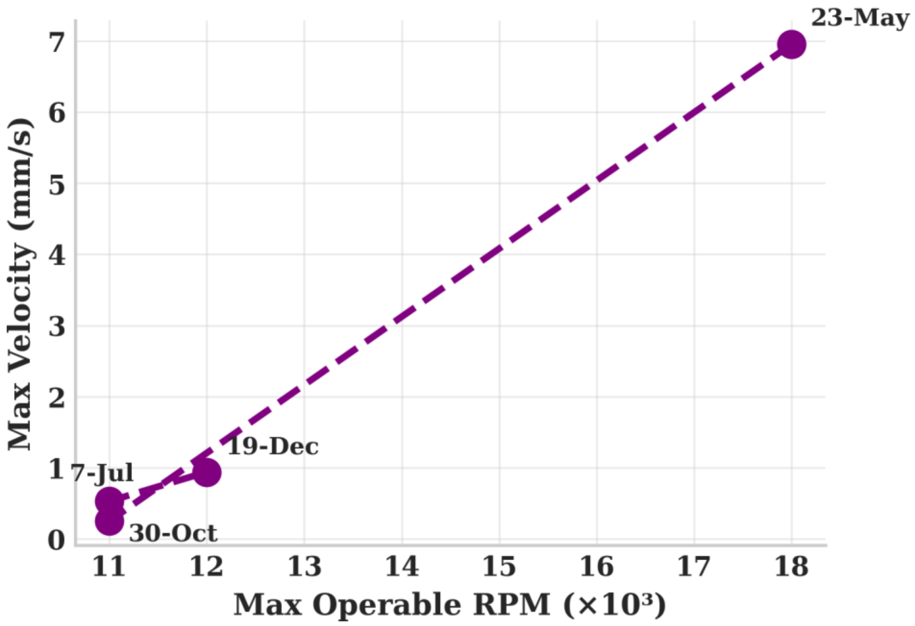


**Figure 18.** Degradation curve.

Figure 18 illustrates the relationship between the degradation of maximum operable spindle speed and vibration velocity. As indicated, between May and July, there is high-speed operation with high vibration levels. This represents early-stage degradation. However, between July and October, there is a decrease in vibration velocity. This represents a phase of operational stability. However, between October and December, there is a sharp increase in vibration velocity. This represents the beginning of accelerated degradation.

This point represents the degradation “knee.” At this point and beyond, failure progression becomes unstable and difficult to predict. However, before this point, maintenance activities can be planned based on trend analysis. After crossing the knee, corrective measures need to be urgently implemented. Thus, the measurements recorded between October and December present a critical early warning phase for undertaking preventive measures.

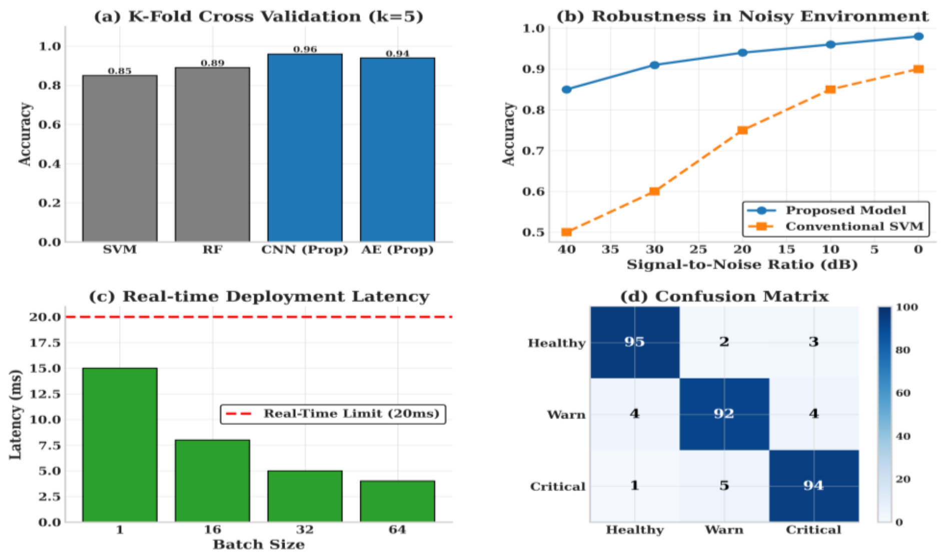


**Figure 19.** Performance validation.

Figure 19 illustrates the effectiveness of the system in terms of several criteria. K-fold cross-validation (Figure 19a) proves the achievement of 96% accuracy, which is an improvement of 11% and 7% over SVM (85%) and RF (89%), respectively, with a low standard deviation of ±2% for the CNN model, which ensures the generality of the model. The noise robustness analysis (Figure 19b) proves the strength of the model in a highly noisy environment, where the CNN model achieves a high accuracy of 98%, compared to SVM, which achieves only 90%, at clean conditions (SNR=40 dB). At moderate noise (SNR=20 dB), the CNN model achieves a high accuracy of 94%, compared to SVM, which achieves only 75%. At very high noise (SNR=0 dB), the CNN model achieves a high accuracy of 85%, compared to SVM, which achieves only 50%. Real-time deployment (Figure 19c) proves the achievement of a latency of 15 ms for a single sample and 5 ms for a batch size of 32, which is within the allowed latency of 20 ms, allowing for the monitoring. The 94% recall for critical faults ensures high safety, with only 6% missed cases. Most errors occur between adjacent health states rather than skipping states, consistent with gradual degradation physics.

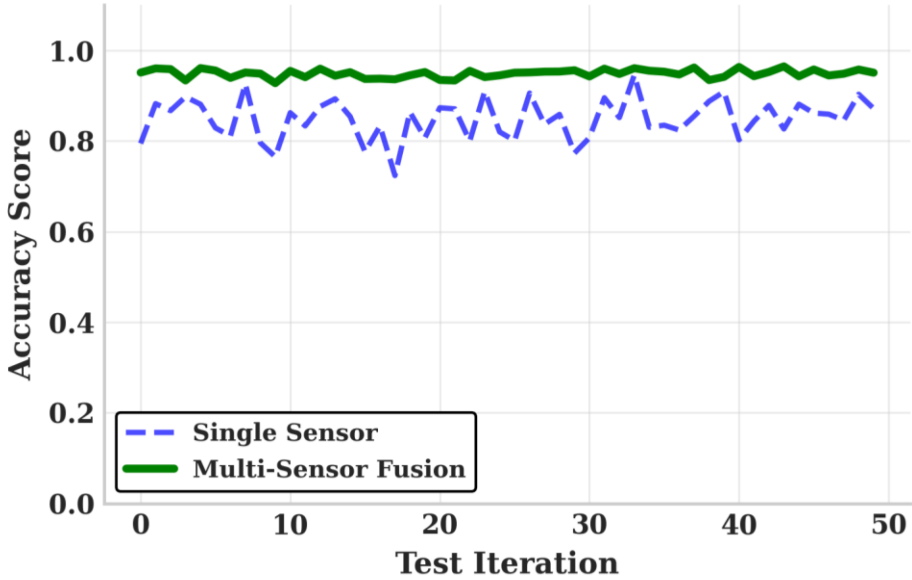


**Figure 20.** Single vs. Multi-sensor fusion.

Figure 20 also validates the multi-sensor fusion technique presented in Section 3.6. The comparison plot shows the accuracy of the diagnostic technique over 50 test iterations for the single sensor technique (blue dashed line) and the proposed multi-sensor fusion technique (green solid line). The accuracy of the proposed multi-sensor fusion technique remains remarkably steady, always above 93%. On the contrary, the accuracy of the single sensor technique varies significantly from 75% to 95%. This shows a high degree of sensitivity to noise or specific operating conditions. The accuracy of the proposed technique is also higher, around 96%, compared to the single sensor technique, which averages around 85%. By using all three sensors, the technique avoids false negatives due to the presence of a specific fault signature, which may be low in one modality and very high in another modality.

Vibration levels increase significantly over time, especially by October and December. Early readings (May–July) are mostly low to moderate, while later readings show sharp rises, especially at mid-range RPMs.

Key Observations by Date:

*23-May (Baseline Condition):* Values mostly between 0.3 – 2.3; Slight increase with RPM (normal behavior); No major spikes; Conclusion: Machine is in good/acceptable condition.

*7-Jul (Early Degradation):* Similar pattern but: Some values slightly higher; A few irregular increases (e.g., around 8000–12000 RPM); Conclusion: Early signs of imbalance or minor misalignment; Still within a monitoring zone.

Preprints.org (www.preprints.org) | NOT PEER-REVIEWED | Posted: 23 April 2026 doi:10.20944/preprints202604.1651.v1



*30-Oct (Significant Change):* Noticeable increases: Peaks around 3–4+; Irregular patternacross RPMs; Not a smooth curve anymore; Conclusion: Likely developing fault; Possible causes: Imbalance worsening; Misalignment; Looseness; Bearing wear starting.

*19-Dec (Critical Condition):* Very high readings: Peaks above 6.0; Strong spikes at multiple RPMs; Highly inconsistent vibration pattern; Conclusion: Machine is in serious condition; Strong indication of: Severe imbalance, Mechanical looseness, Bearing damage, Possible resonance amplification.

**Table 1.** – The results of *g* and *gE* monitoring in a few months.

| 23-May | | | 7-Jul | | 30-Oct | | | 19-Dec | |
|---|---|---|---|---|---|---|---|---|---|
| RPM | *radial g* | *radial gE* | *radial g* | *radial gE* | RPM | *radial g* | *radial gE* | *radial g* | *radial gE* |
| 2000 | 0.43 | 0.29 | 0.13 | 0.22 | 2000 | 0.83 | 0.25 | 0.7 | 0.36 |
| 3000 | 0.82 | 0.44 | 0.15 | 0.44 | 3000 | 0.84 | 0.53 | 2.3 | 0.7 |
| 4000 | 1.41 | 0.68 | 0.18 | 0.53 | 4000 | 2.12 | 0.76 | 4.69 | 1.46 |
| 5000 | 1.8 | 0.65 | 0.14 | 0.49 | 5000 | 2.18 | 0.69 | 5.22 | 1.15 |
| 6000 | 1.52 | 0.62 | 0.27 | 0.53 | 6000 | 3.04 | 0.65 | 5.87 | 1.68 |
| 7000 | 2.06 | 0.52 | 1.66 | 0.43 | 7000 | 3.65 | 0.64 | 6.51 | 1.52 |
| 8000 | 2.08 | 0.6 | 1.61 | 0.48 | 7500 | 4.09 | 0.7 | 5.09 | 1.32 |
| 9000 | 1.76 | 0.49 | 1.42 | 0.38 | 8000 | 4.23 | 0.64 | 5.37 | 1.72 |
| 10000 | 2.38 | 0.42 | 1.89 | 0.36 | 8500 | 4.74 | 0.82 | 5.5 | 1.79 |
| 11000 | 1.59 | 0.5 | 1.36 | 0.35 | 9000 | 4.08 | 0.69 | 5.14 | 1.3 |
| 12000 | 2.01 | 0.4 | 1.77 | 0.31 | 9500 | 4.82 | 0.54 | 6.3 | 0.66 |
| 13000 | 2.03 | 0.36 | 1.35 | 0.27 | 10000 | 5.01 | 0.36 | 4.8 | 0.99 |
| 14000 | 1.84 | 0.45 | 1.63 | 0.3 | 10500 | | | 5.14 | 1.48 |
| 15000 | 2.3 | 0.39 | 1.91 | 0.26 | 11000 | | | | |
| 16000 | 1.46 | 0.31 | 1.05 | 0.23 | | | | | |
| 17000 | 2.23 | 0.3 | | | | | | | |
| 18000 | 1.89 | 0.5 | | | | | | | |
| 19000 | | | | | | | | | |
| 20000 | | | | | | | | | |

**RPM-Based Behavior:** *Low RPM (2000–4000):* Gradual increase over time; Indicates system-wide degradation; *Mid RPM (5000–9000):* Highest vibration spikes in Dec; Suggests: Resonance zone; Structural or alignment issue**;** *High RPM (>9000):* Fluctuating but elevated; Possible: Instability; Dynamic imbalance.

**Critical Red Flags:** Rapid increase between July → October**;** Extreme spikes in December**;** Non-linear vibration pattern → indicates fault progression, not just imbalance.

Likely Root Causes, based on vibration characteristics: *Most Probable***:** Rotor imbalance; Shaft misalignment. *Also Possible:* Bearing degradation; Mechanical looseness; Resonance condition. **Immediate Actions:** Perform full vibration spectrum analysis (FFT); Inspect: Bearings; Coupling alignment; Mounting bolts; Check for looseness. **Maintenance:** Dynamic balancing; Laser alignment; Replace worn components if needed. **Monitoring:** Increase frequency of measurements; Set alarm thresholds. **Final Conclusion:** The machine condition evolved from **normal → warning → critical.** By **December**, the vibration levels indicate **urgent maintenance is required;** Continuing operation may lead to **failure or damage.**

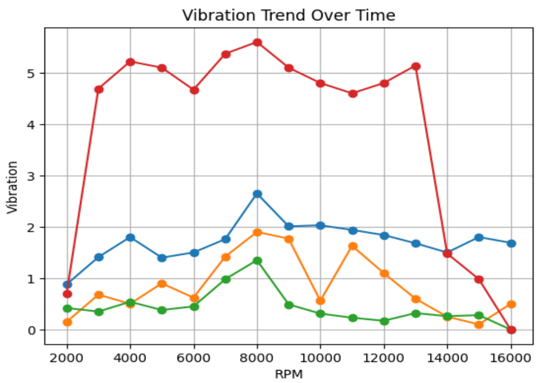


**Figure 14.** Trend of the vibration between May and December.

*Fault Identification (Based on Plot):* Dominant Pattern: Severe Imbalance + Resonance. The December (red curve) shows: Very high vibration in mid-RPM range (3000–13000); A broad peak, not a single spike; This is classic rotating imbalance amplified by resonance. Resonance Zone Detected: Strong amplification between ~4000 and 12000 RPM. This suggests: Natural frequency of the system lies in this range; the machine is hitting a critical speed band.

*Progression Pattern (Important):* May → July: Slight increase → initial imbalance or looseness; July → October: Irregular drop in some areas (possible temporary condition change); Still unstable → developing mechanical issue; October → December: Sudden large amplification; Indicates: Fault crossed threshold; System entered resonance with defect present;

*Secondary Fault Indicators:* Possible Misalignment because: Vibration is not purely proportional to RPM; Curve is not smooth: Possible Mechanical Looseness due to:

Wide-band high vibration (not a sharp peak); Sudden drop at high RPM (loss of stiffness effect); Possible Bearing Wear (early stage)- Not dominant, but contributing. Contributing Factors: Misalignment, Mechanical looseness.

December values (>5) = CRITICAL ZONE, according to industrial standards (e.g., ISO 10816): This is unsafe for continuous operation. In this situation is necessary to do the following activities: (i) Dynamic Balancing (URGENT), this is the main fix; (ii) Check for resonance: Run-up / coast-down test; Identify critical speed precisely; (iii) Alignment Check: Use laser alignment tools; (iv)Tightness Inspection: Foundation bolts; Couplings; Bearings housing; (v) Bearing Inspection: Look for wear or damage.

Critical Speed (Resonance RPM), from the plotted December curve (red): Peak Region:

Vibration sharply rises starting ~3000 RPM; Stays very high until ~13000 RPM; Peak values around: 7000–9000 RPM (~5.5–5.6 max); Estimated Critical Speed: primary resonance ≈ 7500–8500 RPM. Top of FormBottom of Form

## 5. Conclusions

This paper considers the use of artificial intelligence techniques in identifying the operating status of spindles directly on the machine tool. This study proposes a deep learning-based approach to spindle health monitoring based on multi sensor vibration signal analysis. The density-based approach allows the algorithm to understand the natural structure of the process data because a spindle operates at different speeds and loads and the data is not grouped in a uniform area. By ignoring isolated points that do not belong to a dense structure, the model becomes more accurate in diagnosing bearing wear. The problem in the case of spindles and motor-spindles is that one parameter may not adequately capture the cause, so there may be situations where the vibration speed is of a low level and the enveloped acceleration shows the characteristics of the defect or vice versa or both parameters.

In order to select data that ensures the convergence of the results after applying the convolutional neural network, CNN, the Base Density Support Vector Machine, BDSVM, data generation algorithm was used. The proposed AI method is based on the analysis of acceleration and synchronous envelope vibrations by demodulating the signal based on the Hilbert transform to identify critical bearing defects and specific defects at high frequencies. Synchronous envelope vibration analysis (SEVA) combines two well-known methods: envelope analysis, in order to detect the impact of defects such as cracks or bearing faults, and synchronous signal processing, which aligns the vibration signal with a phase reference or shaft rotation, to better isolate periodic components. The novelty of this work lies in the integration of the synchronous envelope analysis method as a support for BDSVM and CNN algorithms in order to provide specific data for closed-loop control of the speed parameter in order to avoid critical vibration zones and increase the spindle life.

The convolutional neural network can learn the features from the raw signal directly, which reduces the need to know the detailed specification of the bearings.

 doi:10.20944/preprints202604.1651.v1



From the results, it can be observed that the proposed approach can monitor the progressive deterioration under different operating conditions. The analysis of the health scores indicates that the deterioration rate is faster when the rotation speed is higher. In addition, the envelope acceleration shows higher sensitivity to the defects in the bearings. The warning, critical, and repair thresholds used in the study are consistent with the ISO 10816 standard, which ensures that the maintenance decisions can be made reliably. Furthermore, the degradation curve analysis shows that there is a "knee" point in the curve, which can serve as an indicator of the unstable operation.

The performance evaluation shows that the approach is robust and efficient in the classification, with 96% accuracy. In addition, the approach is less sensitive to the presence of noise, with less latency in the inference process. The approach can classify the critical faults with a high recall rate. The future direction of the research is to extend the approach for a variety of machine types, online learning, explainability, and the integration of the prediction of the remaining useful life. In the future, research will continue to improve the model of intelligent spindles, integrating thermal system control, tool condition monitoring, and control in addition to vibrations.

## 6. Future work

This section is not mandatory but may be added if there are patents resulting from the work reported in this manuscript.

**Author Contributions:** Conceptualization, C.B., M.W. and A.O.; methodology, C.B.,A.O., S.O., N.M., H.W.; software, C.B.,A.O., S.O., H.W.; validation , C.B., H.W., S.O.; formal analysis, C.B., A.O., H.W., M.N; investigation, C.B., H.W.; resources, C.B., S.O., N.M.; data curation, C.B., H.W.; writing—original draft preparation, C.B.,A.O., H.W.; writing—review and editing, C.B.,A.O.,S.O., H.W.; visualization, H.W.; supervision, C.B., A.O.; project administration, C.B., A.O., S.O., M.N, H.W.; funding acquisition, A.O., C.B., M.N. All authors have read and agreed to the published version of the manuscript.

**Institutional Review Board Statement:** Not applicable.

**Informed Consent Statement:** Not applicable.

**Acknowledgments:** The authors thank you for the support of the Canadian private company TechnoAccord, Leuval.

**Conflicts of Interest:** The authors declare no conflicts of interest.

## References

1. Cao H, Holkup T, Altintas Y. A comparative study on the dynamics of high speed spindles with respect to different preload mechanisms. *Int. J. Adv. Manuf. Technol.* 2011, *57*, 871–883. https://doi.org/10.1007/s00170-011-3356-9.
2. Shokrani , P.J. Arrazola, D. Biermann, P. Mativenga , I.S. Jawahir, Sustainable machining: Recent technological advances, CIRP Annals- Manufacturing Technology 73, 2024, 483-508, https://doi.org/10.1016/j.cirp.2024.06.001.
3. Claudiu BISU, Miron ZAPCIU. In-situ Spindle Diagnostic with Automated Fault Defects Integration. In Proceedings of the 18th CIRP Conference on Intelligent Computation in Manufacturing Engineering, Gulf of Napoli, Italy, 10–12 July 2024, Procedia CIRP, 138, 2026, 222–227, https://doi.org/10.1016/j.procir.2026.01.039.
4. Soori M, Arezoo B, Dastres R. Machine learning and artificial intelligence in CNC machine tools, A review. *Sustain. Manuf. Serv. Econ.* 2023, *2*, 100009. https://doi.org/10.1016/j.smse.2023.100009.
5. Chin, P.; DePavia, J.M.; Veldhuis, S.C. Practical Estimation of Machine Tool Spindle Dynamics for Maintenance Decision Making. *Appl. Sci.* 2024, *14*, 4266. https://doi.org/10.3390/app14104266.
6. Tai, C.Y.; Altintas, Y. A hybrid physics and data-driven model for spindle fault detection. *CIRP Ann. — Manuf. Technol.* 2023, *72*, 297–300.

Preprints.org (www.preprints.org) | NOT PEER-REVIEWED | Posted: 23 April 2026 doi:10.20944/preprints202604.1651.v1




7. Li, X.; Wang, J.; Wang, J.; Wang, J.; Liu, J.; Chen, J.; Yu, X. Research on CNC Machine Tool Spindle Fault Diagnosis Method Based on Deep Residual Shrinkage Network with Dynamic Convolution and Selective Kernel Attention Model. Algorithms 2025, 18, 569. https:// doi.org/10.3390/a1809056
8. Li, X.; Wang, J.; Wang, J.; Wang, J.; Chen, J.; Yu, X. Research on CNCMachineTool Spindle Fault Diagnosis Method Based on DRSN GCEModel. Algorithms 2025, 18, 304. https://doi.org/10.3390/a18060304.
9. Xiangming Zhang, Zhimin Ma, Miaofeng Fang , Yongcan Tang, Jiawei Xiang, Yongying Jiang, Fault diagnosis of motorized spindle based on lumped parameter model and Wasserstein generative adversarial network, Mechanical Systems and Signal Processing 230, 2025, 112668, doi.org/10.1016/j.ymssp.2025.112668.
10. Hongrui Cao, Xingwu Zhanga, Xuefeng Chen, The concept and progress of intelligent spindles: A review, International Journal of Machine Tools & Manufacture, Volume 112, January 2017, Pages 21-52, doi.org/10.1016/j.ijmachtools.2016.10.005.
11. S. Mekid, P. Pruschek, J. Hernandez, Beyond intelligent manufacturing: a new generation of flexible intelligent NC machines, Mech. Mach. Theory 44 (2009) 466–476.
12. Chung-Yu Tai, Yusuf Altintas, Ahybrid physics and data-driven model for spindle fault detection, CIRP Annals- Manufacturing Technology, 72, 2023, 297-300, doi.org/10.1016/j.cirp.2023.04.054.
13. J. Lee, H.-A. Kao, S. Yang, Service innovation and smart analytics for Industry 4.0 and big data environment, Procedia CIRP 16 (2014) 3–8.
14. S. Atluru, S.H. Huang, J.P. Snyder, A smart machine supervisory system frame- work, Int. J. Adv. Manuf. Technol. 58 (2012) 563–572.
15. J. Monnin, F. Kuster, K. Wegener, Optimal control for chatter mitigation in milling-Part 1: modeling and control design, Control Eng. Pract. 24 (2014) 156–166.
16. L. Zhang, R. Yan, R.X. Gao, K. Lee, Design of a real-time spindle health monitoring and diagnosis system based on open systems architecture, in: Proceedings of the International Smart Machining Systems Conference, France, 2007, pp. 373–378.
17. T.L. Schmitz, Chatter recognition by a statistical evaluation of the synchronously sampled audio signal, J. Sound Vib. 262 (2003) 721–730.
18. Bisu C, Zapciu, M Gârleanu, D, Real-Time Envelope Monitoring of High-Speed Spindle in Commissioning Conditions: Grinding Machine, J. Manuf. Mater. Process. 2025, 9, 298. https://doi.org/10.3390/ jmmp9090298.
19. Godreau V, Ritou M, de Castelbajac C, Furet B. Benoit Furet, Diagnosis of spindle failure by unsupervised machine learning from in-process monitoring data in machining. *Int. J. Adv. Manuf. Technol.* **2024**, *131*, 749–759.
20. Louis Oh, Emil Pitz,Kishore Pochiraju, Spindle Condition Monitoring With a Smart Vibration Sensor and an Optimized Deep Neural Network, ASME J Nondestructive Evaluation. May 2023, 6(2): 021003, https://doi.org/10.1115/1.4056616.
21. Weizheng Chen , Zhaojun Yang, Zu'an Ding, Identifying and evaluating spindle tool-tip dynamic response under different workloads, Mechanical Systems and Signal Processing, Volume 185, 15 February 2023, 109728, https://doi.org/10.1016/j.ymssp.2022.109728.
22. Bisu, C.F.; Zapciu, M.; Cahuc, O.; Gérard, A.; Anica, M. Envelope dynamic analysis: A new approach for milling process monitoring. *Int. J. Adv. Manuf. Technol.* **2012**, *62*, 471–486.
23. Feldman, M. Hilbert transform in vibration analysis. *Mech. Syst. Signal Process.* **2011**, *25*, 735–802.
24. Bisu, C.; Olaru, A.; Olaru, S.; Alexei, A.; Mihai, N.; Ushaq, H. Monitoring the Wear Trends in Wind Turbines by Tracking Fourier Vibration Spectra and Density Based Support Vector Machines. *Mathematics* **2024**, *12*, 1307.